Process Biochemistry 43 (2008) 1345–1351

Contents lists available at ScienceDirect

Process Biochemistry

journal homepage: www.elsevier.com/locate/procbio

Induction kinetics of aerobic toluene degradation as a function of carbon starvation history

Joonhong Park [a,*], John Lang [b,e], Kaliannan Thamaraiselvi [a,c], Jerome J. Kukor [d], Linda M. Abriola [e]

[a] School of Civil and Environmental Engineering, Yonsei University, Shinchon-dong 134, Seoul 120-749, Republic of Korea
[b] Environmental and Water Resources Engineering, Department of Civil and Environmental Engineering, The University of Michigan, 181 EWRE Building, 1351 Beal Avenue, Ann Arbor, MI 48109-2125, United States
[c] Department of Environmental Biotechnology, School of Environmental Sciences, Bharathidasan University, Tiruchirappalli 620024, Tamil Nadu, India
[d] Biotechnology Center for Agriculture and the Environment and Department of Environmental Sciences, Rutgers – The State University of New Jersey, 316 Foran Hall, Cook College Campus, 59 Dudley Road, New Brunswick NJ 08901-8520, United States
[e] Department of Civil and Environmental Engineering, Tufts University, 105 Anderson Hall, Medford, MA 02155, United States

ARTICLE INFO

Article history:
Received 24 April 2008
Received in revised form 26 July 2008
Accepted 5 August 2008

Keywords:
Induction kinetics
Carbon starvation
Porous media
Toluene monooxygenase
Biodegradation modeling
Bioremediation

ABSTRACT

In this study, the effects of carbon starvation history on the induction kinetics of aerobic toluene degradation by *Ralstonia pickettii* PKO1 were quantitatively explored. Experimental results suggested that (i) the durations of the lag and transient phases depended upon both the duration of prior carbon starvation (T_{stv}) and the inducer concentration, and (ii) that post-transient-phase (PTP) induction levels were independent of T_{stv} but dependent upon inducer concentration. The observed relationships among toluene degradation, carbon starvation history, and inducer concentration were incorporated into a modified Michaelis–Menten equation in order to refine the traditional model of enzymatic biodegradation. The refined model was able to predict toluene breakthrough in a porous medium in which previously carbon-starved cells were reactivated with a continuous supply of toluene. These findings suggested a means of improving the accuracy of existing models of biodegradation in groundwater under conditions of fluctuating substrate/inducer concentration.

1. Introduction

A variety of aromatic and aliphatic bacterial oxygenases are capable of breaking down trichloroethene (TCE), a widespread contaminant of soil and groundwater, under aerobic conditions [1–10]. Utilization of such oxygenase-expressing bacteria for *in situ* biodegradation of TCE is a promising strategy for environmental remediation. Bacteria such as *Burkholderia* sp. strain G4 and *Ralstonia pickettii* PKO1 that express toluene monooxygenase (TMO) are of particular interest because they are resistant to TCE-mediated toxicity [11,12]. Furthermore, when toluene was added to polluted sites in order to stimulate subsurface TCE-cooxidation, TMO-containing bacteria were identified as a major aromatic-degrading population [13,14].

When the concentration of an essential nutrient, such as a carbon source, energy source, or electron acceptor, is below its threshold, a microorganism that was previously engaged in exponential growth may enter into a non-growth phase, such as stationary or death phase [15]. In heterotrophic bacteria, a group to which most microbes capable of biodegradation belong, the depletion of energy and carbon sources (primary substrates) induces proteomic and genomic responses within the organism [16–18]. Carbon starvation also affects microbial adhesion and aggregation. The extracellular polysaccharides responsible for structural integrity and hydrophobicity may also facilitate microbial adhesion and aggregation, and the induction of biofilm formation in response to starvation conditions has been demonstrated [19]. Furthermore, the kinetics of microbial growth on aromatic hydrocarbons has been shown to be influenced by the microbe's carbon starvation history [20]. Since subsurface microbes, which are believed to exist primarily in an attached state [21,22], are often encountered in dormant or starved states [15], carbon starvation may have a significant impact on the ability of these organisms to bioremediate soil and groundwater [23].

In TCE-cooxidizing bacteria, carbon starvation conditions deactivate toluene oxygenase [24–26]. The deactivation rate of TMO-containing TCE-degrading microbes was found to be more than an order of magnitude greater than that of other oxygenase-containing bacteria [27]. Supplying the TCE-cooxidizing bacteria with a primary substrate for cellular growth and a chemical inducer of the TMO

* Corresponding author. Fax: +82 2 2 364 5300.
E-mail address: parkj@yonsei.ac.kr (J. Park).

1359-5113/$ – see front matter © 2008 Elsevier Ltd All rights reserved.
doi:10.1016/j.procbio.2008.08.004

pathway can restore TMO activity to previously deactivated cells [28,29]. These findings suggested that induction kinetics may be crucial to predicting biodegradation rates accurately. However, quantitative information regarding the induction kinetics of biodegradation is limited, particularly with respect to an organism's carbon starvation history or the concentration of substrate/inducer present.

Our previous experiment with *R. pickettii* PKO1 [29] indicated that the traditional Michaelis–Menten and Monod models were unable to predict the rate of aerobic toluene degradation under conditions of fluctuating substrate/inducer (toluene) concentrations in porous media. A new quantitative framework was required to describe the induction kinetics of aerobic biodegradation as a function of both the organism's history and the concentration of substrate/inducer present. The main objective of this study was to quantify and model the induction kinetics of aerobic biodegradation in response to carbon starvation and substrate/inducer concentration. To this end, the durations of the lag and transient periods of oxygenase activity and induction levels were related to the duration of prior carbon starvation and to the concentration of substrate/inducer present. Based upon these data, a quantitative framework describing the observed induction kinetics was proposed and used to refine the traditional model of enzymatic biodegradation. We then tested the refined model's validity by comparing its predictions for column toluene degradation under conditions of fluctuating substrate/inducer concentration to previously reported experimental data [29].

2. Materials and methods

2.1. Materials

A basal salt medium (BM [30]) was used for minimal mineral medium, and tryptone nutrient agar (TNA [31]) served as the solid growth medium. Spectrophotometric-grade TCE (Fisher Scientific Co.) and HPLC-grade toluene (Aldrich Chemical Co.) were used. Sodium DL-lactate (Fisher Scientific Co.) served as both a carbon and an energy source for *R. pickettii* PKO1.

2.2. Preparation of toluene-grown and carbon-starved cells

Prior to carbon starvation, cells were grown in a 4-L culture flask containing 500 mL BM and whose headspace was saturated with toluene vapor. In order to ensure continuous toluene vapor saturation and adequate enzymatic induction, a 1.8 mL GC vial filled with 0.5 mL of liquid toluene was suspended above the liquid medium inside each 4-L culture flask. The concentration of toluene dissolved in the liquid BM was estimated to be approximately 230 mg/L. The culture flasks were incubated while shaking at 250 rpm at 30 °C for 72 h. The cells were then harvested from the spent medium by centrifugation (9264 × *g* at 4 °C for 10 min). Prior to use, the pelleted cells were washed with fresh BM and subsequently resuspended in 50 mL of fresh BM. Carbon-starved cells were prepared in 50 mL of carbon-free medium in 500 mL culture flasks, which were stirred with a magnetic stirrer at 120 rpm to improve mixing and aeration. The cells were incubated in a laminar airflow chamber at room temperature for a specific period of carbon starvation.

2.3. Analytical techniques

A plate count method [29] was employed to quantify viable biomass. Toluene concentration was measured using a Hewlett-Packard 1090 series II HPLC system equipped with a reverse-phase hypersil $5C_{18}$ column and a UV (210 nm) detector. For HPLC analysis, 0.5 mL aliquots were removed from culture using airtight 1-mL micro-syringes, mixed with an equal volume of methanol in a 1.8-mL GC vials, and stored at 4 °C.

2.4. Measurement of the specific activity of toluene degradation

The initial rate of toluene degradation was measured and then normalized to the viable biomass to yield the specific activity of toluene degradation. Prior to measurement, cells were harvested, pelleted, washed, resuspended in BM, and pre-oxygenated for 30 min. Completely mixed 15-mL batch reactors equipped with sampling ports sealed with GC (gas-chromatograph) septa (Alltech Associates, Inc.) were used as previously described [29]. The reactors were completely filled with the pre-oxygenated cell suspensions, leaving no remaining headspace, and then crimp-sealed. A predetermined amount of a stock solution of toluene in *N*′,*N*′-dimethylformamide through each reactor's GC-septum such that the initial aqueous concentration of toluene was 5 mg/L. The disappearance of toluene was monitored either every 15 min for 1 h or every 30 min for 2 h.

2.5. Characterization of induction kinetics

When carbon-starved cells were reactivated with toluene, lag times and transient periods were measured as a function of variations in carbon starvation history and toluene concentration. Cell suspensions (10 mL) that had been carbon-starved for varying durations of time (T_{stv} = 0, 2.75, 7.15, and 14 d) were added to 160-mL serum bottles, and varying amounts of toluene were added to each of the bottles such that the final toluene concentration was 0.6, 1.4, 3.5, 6.0, or 12.0 mg/L. A modified protocol for toluene degradation assays in 160-mL serum bottles [29] was employed for the reactivation experiments. Under these conditions, the effects of artifacts on the lag and transient phases were negligible. Lag times of only 2–5 min were observed for both toluene-induced and resting cell samples. The initial density of living cells in each serum bottle was adjusted to approximately 10^8 cfu/mL (equivalent to 58 mg-wet cell mass/L) in order to ensure cell concentrations sufficient to accurately measure the rate of toluene degradation. Following the addition of toluene, the serum bottles were incubated at 24 ± 2 °C with shaking at 250 rpm, and the toluene disappearance was monitored.

The lag time (L) was defined as the amount of time between toluene injection and the point at which the extent of toluene disappearance had exceeded the detection limit of the measurement apparatus (approx. 0.1 mg/L aqueous toluene). For example, in Fig. 1a, the lag time was measured as 3 h. The length of the transient period (TP) was defined as the time between the end of the lag phase and the point at which maximal rate of biodegradation was reached. For example, in Fig. 1b, the maximal degradation rate was observed at 6.7 h post-injection, and so the length of TP was calculated to be 3.7 h by subtracting the observed lag time (3 h) from this value of 6.7 h. Degradation rates were calculated based upon toluene mass balance taking into account the equilibrium partitioning of toluene between the gaseous (150 mL) and aqueous phases (10 mL) in each 160-mL serum bottle. For this calculation, the dimensionless Henry constant for toluene was assumed to be 0.243 at 25 °C [32].

The effect of the duration of carbon starvation on the induction kinetics of the TMO pathway was characterized using cells that had been starved for varying lengths of time (0, 2, 7 and 21 d). These cells were reactivated with a solution of lactate and TCE (110 mg/L). TCE induction was monitored by measuring the specific

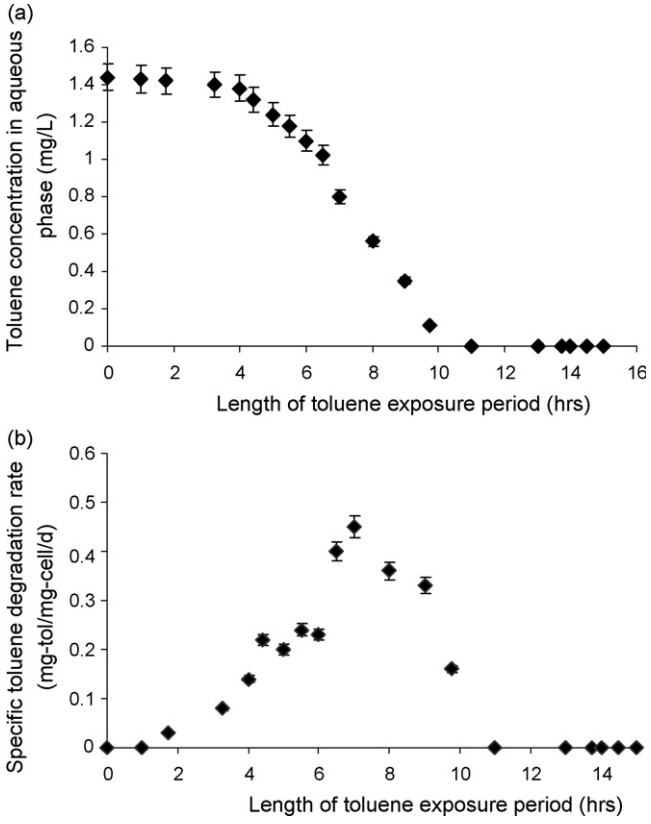

Fig. 1. Time course of (a) the disappearance of toluene and (b) the corresponding specific rate of toluene degradation corresponding to cells that were reactivated with 1.44 mg/L toluene following carbon-starvation for 2.75 days. *Y*-axis error bars correspond to one standard deviation of independent replicate experiments.

rate of toluene degradation. The detailed protocol used for these reactivation experiments is described elsewhere [12]. In the TCE-lactate reactivation system, TCE is the sole inducer of toluene degradation in *R. pickettii PKO1*, while lactate is the growth substrate [12]. TCE is an established inducer of the TMO pathway in this strain [30,33], and the mechanism of TCE induction is described elsewhere [34]. Unlike a toluene-based reactivation system, the TCE-lactate reactivation decouples the inducer's effects from those of the growth substrate while simultaneously keeping the inducer (TCE) concentration fairly constant.

The effect of inducer concentration on post-transient-phase (PTP) induction was also examined. The specific activity of toluene degradation was measured for cells induced with varying initial concentrations of either toluene or TCE.

3. Results and discussion

3.1. Lag and transient phases

Carbon starvation batch experiments were conducted to measure the lag time of toluene degradation activity induction (Fig. 2a). The duration of the lag period (L) increased with increasing prior carbon starvation (T_{stv}), up to T_{stv} = 7 days, before reaching a plateau. The observed lag time was attributed to microbial environmental acclimation, specifically the preparation of the necessary toluene-degrading metabolic enzymes [35]. During the transient phase, global physiological adjustments, aimed at altering the whole cells' degradation capabilities, are generally achieved through changes in transcriptional expressions and enzymatic induction [35]. The lag time (L) and transient period (TP) data demonstrated that the lengths of both of the corresponding phases responded similarly to variations in the duration of prior carbon starvation, T_{stv} (Fig. 2b).

The apparent effect of carbon starvation history on the durations of the lag phase and transient periods was attributed to the greater sensitivity of more thoroughly starved cells to toluene-mediated stress [11]. Toluene is a hydrophobic solvent known to disturb the outer and cytoplasmic membranes of bacteria [36]. While toluene-grown and non-starved PKO1 cells exhibit neither lag nor transient phases [12], the durations of the lag and transient phases in starved PKO1 cells increased more sensitively to increasing toluene concentrations (Fig. 2). These findings suggested that the cells' defensive mechanism(s) against toluene-mediated stress may depend on the energy-state or growth-phase of the organism.

3.2. Effects of carbon starvation history on induction kinetics

Results from the TCE-lactate reactivation experiments provided information regarding the effects of carbon starvation history (i.e., the duration of the previous period of carbon starvation, T_{stv}) on the induction kinetics of toluene degradation by PKO1. The durations of the TCE-induced cultures' lag and transient phases appeared to increase with increasing T_{stv} (Fig. 3), and this finding was consistent with the previous observations regarding toluene-induced cells (Fig. 2).

A significant lag time (approximately 40 min) was observed when cells grown on lactate were exposed to TCE (Fig. 3). Because growth on lactate does not induce the production of the TMO enzyme in PKO1 cells [12], the observed lag time was attributed to the time necessary for the cells to accumulate the enzymes of the toluene degradation pathway in response to the TCE inducer. In addition, in the lactate-grown cells, the lag time following TCE induction was longer than that following toluene induction (less than 15 min). Thus, this finding suggested that TCE is more toxic to PKO1 cells than toluene. In TMO-expressing bacteria, the toxic effects of exposure to TCE are two-fold. First, the degradation of TCE generates toxic byproducts, and, second, TCE itself can be responsible for solvent-mediated toxicity [12]. Exposure to toluene only causes solvent-mediated toxicity.

As the duration of prior carbon starvation was increased, the increase in the specific rate of toluene degradation over the transient period exhibited greater non-linearity (Fig. 3). When

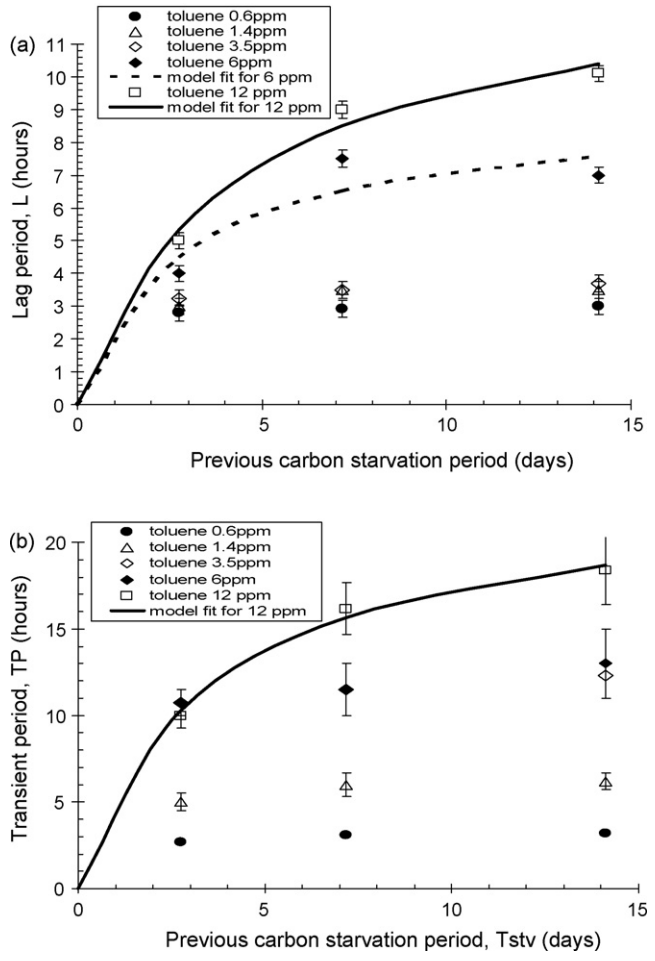

Fig. 2. (a) The duration of lag phase (L) as a function of the duration of prior carbon starvation (T_{stv}). (b) The duration of the transient phase (TP) as a function of T_{stv}. Boxed values indicate the initial toluene concentrations used during reactivation experiments. Lines correspond model fitting results.

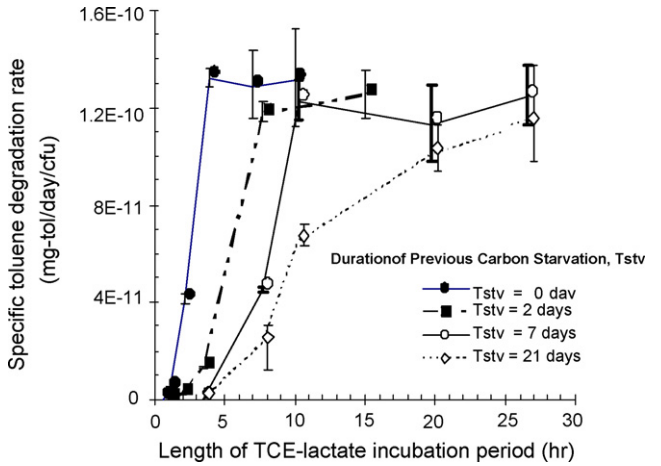

Fig. 3. Time courses of the specific rate of toluene degradation during reactivation with TCE (110 mg/L).

lactate-grown cells were exposed to TCE (T_{stv} = 0 day), the degradation rate rapidly increased in a linear manner to its maximal value (1.3×10^{-10} mg toluene/day/cfu). In contrast, for cells starved for 21 days induction of toluene degradation was much slower and exhibited a more sigmoidal trend during the transient phase. These results also indicated that as cells were starved for longer periods they became more sensitive to TCE-mediated toxicity.

Despite the susceptibility of starved cells to TCE-mediated toxicity, the duration of carbon starvation did not significantly affect the post-transient-phase (PTP) rate of toluene degradation (i.e., plateaued rates in Fig. 3). If the PTP rate of degradation had also been dependent upon carbon starvation history, then this would have significantly complicated subsequent kinetic modeling of toluene biodegradation. Fortunately, this was not the case. Nevertheless, carbon starvation history did affect the durations of the lag and transient phases. These results suggested that the organism may contain energy-state or growth-phase dependent defensive mechanism(s) against TCE-mediated toxicity [12].

3.3. Effects of inducer concentration on post-transient-phase (PTP) degradation rate

When the aerobic toluene degradation activity of previously carbon-starved cells was reactivated with either TCE or toluene, the PTP steady-state rate of toluene degradation was dependent upon the concentration of inducer present (Fig. 4). Compared to the steady-state degradation rates of TCE-induced cells, those of toluene-induced cells plateaued at much lower inducer concentrations (~10 mg/L toluene vs. >550 mg/L TCE). In addition, the maximal rate of toluene degradation following toluene induction was approximately 4 times greater than that following TCE induction. Thus, toluene was a much more potent and effective inducer of toluene degradation than TCE. A reduced rate of net TCE uptake through outer and cytoplasmic membranes as a result of the compound's toxicity could have been partly responsible for this effect. Alternatively, TCE was simply a less potent than toluene with respect to activating transcriptional regulation of TMO expression [34]. Although the exact mechanism was not yet determined, these results nevertheless indicated that the toxicity and/or chemical structure of a compound can significantly affect its potency and efficacy as a chemical inducer.

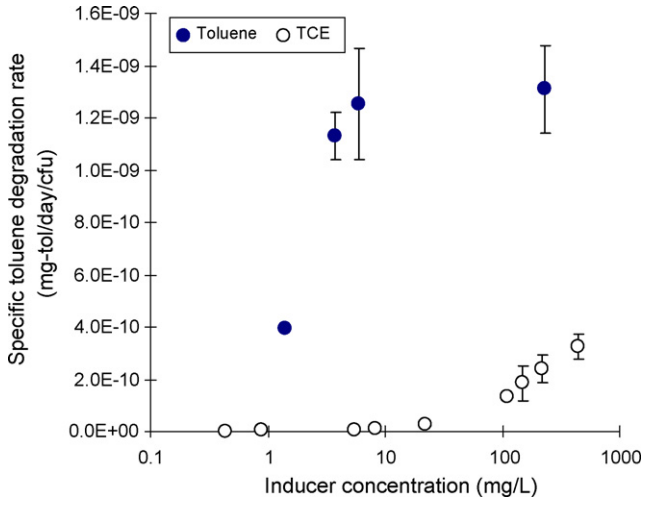

Fig. 4. Specific rate of toluene degradation as a function of inducer concentration (toluene and trichloroethylene).

3.4. Refining the existing biodegradation model

A novel quantitative framework for modeling toluene biodegradation was proposed to refine the conventional Michaelis–Menten and Monod kinetic models to reflect the effects of substrate/inducer exposure and starvation history on induction kinetics. This model was constructed based upon the results from the reactivation experiments conducted using toluene rather than those using TCE (Figs. 2 and 4), because the kinetics and toxicity of toluene induction were more ideal than those of TCE induction. Because toluene simultaneously serves as both a substrate for cell growth and an inducer of biodegradation pathways in many TMO-expressing bacteria, this property of the substrate/inducer compound (C) was incorporated into the model's assumptions. Based upon the previous experimental data (Fig. 2), it was assumed that when previously starved cells were reactivated via substrate/inducer exposure, the durations of the lag and transient phases depended upon both the duration of prior carbon starvation (T_{stv}) and the initial concentration of the substrate/inducer compound (C). Hyperbolic equations were used to describe the relationships among T_{stv}, L, and TP (Eqs. (1a) and (2a)).

$$\text{Lag time, } L = \frac{L_{max}(C) \cdot T_{stv}}{T_M^{lag}(C) + T_{stv}} \qquad (C > C_{th\text{-}IND}) \tag{1a}$$

$$L = \infty \qquad (C \le C_{th\text{-}IND}) \tag{1b}$$

$$\text{Transient phase, } TP = \frac{TP_{max}(C) \cdot T_{stv}}{T_M^{trans}(C) + T_{stv}} \qquad (C > C_{th\text{-}IND}) \tag{2a}$$

$$TP = \infty \qquad (C \le C_{th\text{-}IND}) \tag{2b}$$

In the equations above, C represents the concentration of substrate/inducer (toluene) $L_{max}(C)$ is the maximum lag time, $TP_{max}(C)$ is the maximal duration of the transient phase, $T_M^{lag}(C)$ is the duration of prior carbon starvation corresponding to 50% of $L_{max}(C)$, and $T_M^{trans}(C)$ is the duration of prior carbon starvation corresponding to 50% of $TP_{max}(C)$. The durations of the lag and transient phases for non-starved cells (T_{stv} = 0) were assumed to be zero. Cases in which the inducer concentration was below the threshold for induction ($C_{th\text{-}IND}$) were designated as "no-induction" and were represented by setting the values of L and TP equal to infinity (Eqs. (1b) and (2b)). These hyperbolic equations were accurately fitted to data from the lag time experiments in which starved deactivated cells were reactivated with toluene (substrate/inducer) concentrations of 6 and 12 mg/L (R^2 = 0.957 and 0.993, respectively). Similarly, these hyperbolic equations were also fitted to the experimental data measuring the duration of the transient phase of cells reactivated with 12 mg/L toluene (R^2 = 0.998). The high correlation coefficients corresponding to these numerical regressions supported the application of these equations for subsequent calculations necessary for modeling. Because both lag time and the duration of the transient phase of starved cells depended upon toluene concentration (Fig. 2), it was assumed that the new model parameters, L_{max}, TP_{max}, $T_M^{lag}(C)$ and $T_M^{trans}(C)$, were also functions of the substrate/inducer concentration, C. However, the available data (Fig. 2) was insufficient for finding a statistically significant correlation between these parameters and toluene concentration.

Another hyperbolic equation (Eq. (3)) was assumed to be a reasonable approximation for describing the relationship between the final steady-state PTP rate of toluene degradation and the substrate/inducer concentration, because the toluene induction

data demonstrated an asymptotic trend (Fig. 4).

$$\frac{I}{I_{MAX}} = \frac{C}{K_{MI} + C} \tag{3}$$

In the equation above, I is induced rate of toluene degradation, I_{MAX} is maximal induced rate of toluene degradation, and K_{MI} is the corresponding half-saturation constant.

A scaling factor (ε) was introduced into the conventional Michaelis–Menten relationship (Eq. (4)), in order to describe the kinetics of induction of toluene degradation in response to carbon starvation history and substrate/inducer exposure. This modification assumed that the maximum specific degradation rate (υ_{max}), but not the half-saturation constant (K_m), was dependent upon the initial substrate/inducer concentration. The assumption was sound unless $K_m \gg C$, because the biodegradation rate was much more sensitive to changes in υ_{max} than to changes in K_m.

$$-\frac{dC}{dt} = \frac{\upsilon_{max} C}{K_m + C} \varepsilon X_m \tag{4}$$

In the above equation, t is time, and X_m is the total biomass present. When TCE-degrading bacteria are exposed to sub-threshold concentration of substrate/inducer such as under carbon starvation conditions, the specific activity of toluene degradation was found to decrease exponentially as the duration of prior carbon starvation was increased [26,27]. A first-order decay expression was therefore employed to express the scaling factor ($\varepsilon_{Down\text{-}shift}$) as a function of the duration of carbon starvation (Eq. (5)).

$$\varepsilon_{Down\text{-}shift} = f(t_{stv}) = EXP(-k_{DA} t_{stv}) \tag{5}$$

In the equation above, t_{stv} represents the duration of time over which the substrate/inducer concentration was below $C_{th\text{-}DA}$, and k_{DA} is the first-order rate constant of deactivation. In TCE-degrading TMO bacteria, the first-order deactivation rate constant was found to be both organism-specific and independent of previous induction history and/or growth conditions [27].

When previously starved, completely deactivated cells are exposed to substrate/inducer concentrations above a specific threshold value, $C_{th\text{-}IND}$ (Up-shift stage), the induction kinetics of toluene degradation are a function of T_{stv}, C, and the duration of the subsequent exposure to substrate/inducer (t_e).

$$\varepsilon_{Up\text{-}shift} = f(T_{stv};\ C;\ t_e) \tag{6}$$

In the equation above, it should be noted that T_{stv} is a fixed value representing a previous event (carbon starvation), while t_e is a time variable for the current event being simulated (reactivation). Three different Eqs. (7a)–(7c) are required to represent the scaling factors as functions of time during the lag, transient, and post-transient-phases.

$$\text{Lag phase}: \varepsilon_{Up\text{-}shift} = 0 \quad (0 \le t_e < L) \tag{7a}$$

$$\text{Transient phase}: \varepsilon_{Up\text{-}shift} = \frac{\varepsilon_{PTP}}{TP}(t_e - L) \qquad (L \le t_e < L + TP) \tag{7b}$$

$$\text{Post transient phase}: \varepsilon_{Up\text{-}shift} = \varepsilon_{PTP} = \frac{C}{[K_{MI} + C]} \quad (L + TP \le t_e) \tag{7c}$$

If toluene degradation activity is completely eliminated prior to reactivation, the $\varepsilon_{Up\text{-}shift}$ value corresponding to the lag phase must be set to zero (Eq. (7a)). The values of L and TP can be calculated from Eqs. (1) and (2). A linear relationship was assumed to be a good approximation for $\varepsilon_{Up\text{-}shift}$ during the transient phase (Eq. (7b)), because during this phase the inducer causes relatively little toxicity relative to its inductive effects upon the TMO pathway. The rate of degradation during the PTP phase, ε_{PTP}, was assumed to be a function of substrate/inducer concentration (C), because experimental results suggested that this rate was dependent upon toluene concentration (Fig. 4).

3.5. Model validation

In order to evaluate the predictive power of the refined biodegradation model, numerical simulations of the behavior of a biodegradation column were performed using independently determined model parameters (Table 1), and the results were compared to experimental results obtained for a similar column biodegradation system [29]. For this evaluation, toluene breakthrough data from our previous study of column biodegradation ([29], Figs. 2 and 5) were used. The scope of the model simulation was limited to the first peak in concentration. The conditions employed during these column experiments was as follows: (i) microbial toluene degradation activity was fully induced with toluene (approximately 230 mg/L in the culture medium) prior to inoculation of a sandy porous medium; (ii) the toluene degradation of the inoculated cells was completely deactivated over a 2.23 d period of carbon starvation in which no toluene was present; and (iii) following deactivation, toluene (1.2–1.3 mg/L) was continuously supplied in the column effluent. A one-dimensional finite-element simulation was implemented using the refined Michaelis–Menten model (Eq. (4)) coupled with the new induction kinetic Eqs. (1), (2), (3) and (7a)–(7c). Advective and dispersive solute transport, equilibrium linear sorption, toluene utilization, and microbial growth and death were all incorporated into this one-dimensional simulation. Model equations were simplified to a coupled system of two differential equations, the following a partial differential equation governing both the transport and transformation of toluene:

$$\left(1 + \frac{\rho_b K_D}{n}\right)\frac{\partial C}{\partial t} = -\frac{\partial}{\partial x}(vC) + \frac{\partial}{\partial x}\left(\alpha_L |v| \frac{\partial C}{\partial x}\right) + \varepsilon\left(\frac{\upsilon_{max} C}{K_m + C}\right)\left(\frac{X_m}{n}\right) \tag{8}$$

and the following ordinary differential equation governing microbial mass balance:

$$\frac{dX_m}{dt} = Y\left(\varepsilon \frac{\upsilon_{max} C}{K_m + C}\right) X_m - b X_m \tag{9}$$

In the equations above, C is the concentration of toluene in the aqueous phase, t is time, x is distance along the column, and X_m is the concentration of viable biomass present in the bulk phase. The other parameters corresponding to Eqs. (8) and (9) are defined in Table 1. The Michaelis–Menten (biotransformation) and Monod (growth) parameters were based upon those measured under batch-suspended-growth conditions [29]. A $C_{th\text{-}IND}$ value of 0.005 mg/L toluene and a K_{MI} value of 0.4 mg/L toluene were determined from transcriptional activation experiments with P*tbu*A1 [37]. The values for L and TP were taken from Fig. 2a (T_{stv} = 2.75 d) and Fig. 2b (C = 1.4 mg/L), respectively, because these values corresponded to the conditions employed during the column degradation experiments.

The simulation predictions were in good agreement with the model predictions and the experimental data. For estimated parameters, all values used for the simulation fell within the error range of these estimates (Table 1). The tailing effect predicted by the simulation was at concentrations close to the detection limit of toluene in the column effluent (0.01 mg/L). These findings

Table 1
Parameters used in the simulation of toluene degradation on a column

Parameter	Average value	95% C.I.*
Maximum specific toluene degradation rate (υ_{max})[a] ($mg_{-toluene}/mg_{-cell}/d$)	2.26	1.82–2.96
Half-saturation toluene concentration (K_m)[a] ($mg_{-toluene}/L$)	1.20	1.17–1.23
Cell yield coefficient (Y)[a] ($mg_{-cell}/mg_{-toluene}$)	0.5	0.4–0.6
Cell decay coefficient (b)[a] (1/d)	0.06	0.03–0.09
Threshold toluene concentration for reactivation ($C_{th\text{-}IND}$)[b] ($mg_{-toluene}/L$)	0.005	<0.01
Length of lag phase (L)[b] (h)	2.9	2.8–3.0
Length of transient phase (TP)[b] (h)	5.0	4.5–5.5
Half-saturation constant of induction (K_{MI})[b] ($mg_{-toluene}/L$)	0.4	0.3–0.5
Initial concentration of biomass in the bulk phase (X_m at $t = 0$)[a] (mg_{-cell}/L)	3.72	2.85–4.60
Interstitial velocity (υ)[a] (cm/h)	1.21	1.20–1.22
Dispersivity (α_L)[a] (cm)	0.18	0.14–0.27
Linear sorption coefficient (K_D)[a] (mL/g)	0.020	0.003–0.039
Porosity (n)[a] dimensionless	0.35	0.34–0.36
Bulk phase column density (ρ_b)[a] (g/mL)	2.03	2.00–2.06

* Indicates 95% confidential interval.
[a] Reported in our previous study [29].
[b] Measured in this study.

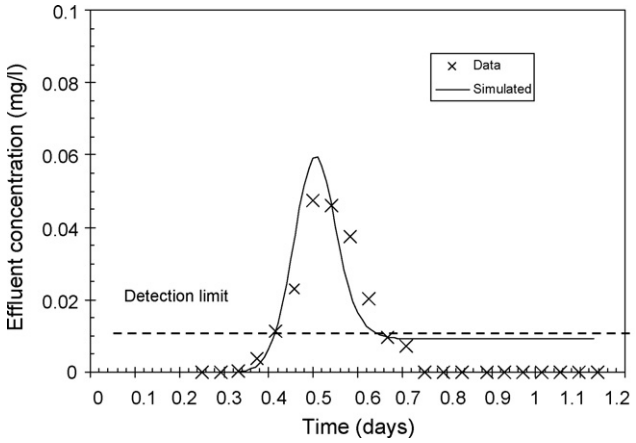

Fig. 5. Simulation prediction (solid line) vs. experimental data (symbols) for toluene breakthrough. The dashed line indicates the lower detection limit for toluene (0.01 mg/L toluene).

demonstrated that the refined biodegradation model could predict the dynamic, history-dependent induction kinetics of toluene degradation under conditions of fluctuating substrate/inducer concentrations.

4. Conclusion

In this study, the effect of carbon starvation history on the induction kinetics of aerobic toluene degradation by *R. pickettii* PKO1 was explored quantitatively. Cells starved of carbon for longer periods of time became more sensitive to the inducer-mediated stresses, including solvent-mediated stress and/or degradation-dependent toxicity. These findings suggested that the organism's defenses against these chemical-mediated stresses may be energy-state or growth-phase dependent, and that this energy-state/growth-phase dependent defensive mechanism might have been responsible for the effect of carbon starvation history on the induction kinetics of toluene degradation in PKO1.

Based upon these experimental observations, a novel model was proposed to describe the induction kinetics of biodegradation as a function of both the biocatalyst's carbon starvation history and the substrate/inducer concentration. Hyperbolic equations were used to describe (i) the durations of the lag and transient phases as functions of T_{stv} and (ii) the asymptotic behavior of the rate of toluene degradation during the PTP as a function of C. These new history-rate relationships were used to refine the traditional Michaelis–Menten model of biodegradation.

The conventional kinetic models based on the Michaelis–Menten and Monod equations are unable to predict the history-dependent induction kinetics of toluene biodegradation. Nevertheless, the good agreement between the simulation's predictions and the experimental measurements of toluene degradation on a column validated the predictive power of the refined model. These findings provide a basis for improving the accuracy of measurements of *in situ* TCE-cooxidation rates under conditions of fluctuating substrate/inducer concentration at bioremediation sites, where carbon starvation conditions are commonplace.

Acknowledgements

This study was supported by Superfund Basic Research Program grant P42-ES-04911 from the National Institute of Environmental Health Sciences of the US National Institute of Health. The study was also supported by a grant from the Basic Research Program (R01-2006-000-10136-0) of the Korea Science & Engineering Foundation.

References

[1] Arciero D, Vanneli T, Logan M, Hooper AB. Degradation of trichloroethylene by the ammonia-oxidizing bacterium *Nitrosomonas europea*. Biochem Biophys Res Commun 1989;159:640–3.
[2] Zylstra GJ, Wackett LP, Gibson DT. Trichloroethylene degradation by *Escherichia coli* containing the cloned *Pseudomonas putida* F1 toluene dioxygenase genes. Appl Environ Microbiol 1989;55:3162–6.
[3] Folsom BR, Chapman PJ, Pritchard PH. Phenol and trichloroethylene degradation by *Pseudomonas cepacia* G4: kinetics and interactions between substrates. App Environ Microbiol 1990;56:1279–85.
[4] Fox BG, Borneman JG, Wackett LP, Lipscomb JD. Haloalkene oxidation by the soluble methane monooxygenase from *Methylosinus trichosporium* OB3b: mechanistic and environmental implications. Biochemistry 1990;29:6419–27.
[5] Whited GM, Gibson DT. Toluene-4-monooxygenase, a three-component enzyme system that catalyzes the oxidation of toluene to *p*-cresol in *Pseudomonas mendocina* KR1. J Bacteriol 1991;173:3010–6.
[6] Ensign SA, Hyman MR, Arp DJ. Cometabolic degradation of chlorinated alkenes by alkene monooxygenase in a propylene-grown *Xanthobacter* strain. Appl Environ Microbiol 1992;58:3038–304.
[7] Heald S, Jenkins RO. Trichloroethylene removal and oxidation toxicity mediated by toluene dioxygenase of *Pseudomonas putida*. Appl Environ Microbiol 1994;60:4634–7.
[8] Malachowsky KJ, Phelps TJ, Teboli AB, Minnikin DE, White DC. Aerobic mineralization of trichloroethylene, vinyl chloride, and aromatic compounds by *Rhodococcus* species. Appl Environ Microbiol 1994;60:542–8.
[9] Olsen RH, Kukor JJ, Kaphammer B. A novel toluene-3monooxygenase pathway cloned from *Pseudomonas pickettii* PKO1. J Bacteriol 1994;176:3749–56.
[10] Lontoh S, Semrau JD. Methane and trichloroethylene degradation by *Methylosinus trichosporium* OB3b expressing particulate methane monoxygenase. Appl Environ Microbiol 1998;64:1106–14.
[11] Mars AE, Houwing J, Dolfing J, Janssen DB. Degradation of toluene and trichloroethylene by *Burkholderia cepacia* G4 in growth-limited fed-batch culture. Appl Environ Microbiol 1996;62:886–91.
[12] Park J, Kukor JJ, Abriola LM. Characterization of the adaptive response to trichloroethylene-mediated stresses in *Ralstonia pickettii* PKO1. Appl Environ Microbiol 2002;68:5231–40.
[13] Hopkins GD, McCarty PL. Field evaluation of in situ aerobic cometabolism of trichloroethylene and three dichloroethylene isomers using phenol and toluene as the primary substrates. Environ Sci Technol 1995;29:1628–37.
[14] McCarty PL, Goltz MN, Hopkins GD, Dolan ME, Allan JP, Kawakami BT, et al. Full-scale evaluation of in situ cometabolic degradation of trichloroethylene in groundwater through toluene injection. Environ Sci Technol 1998;32:88–100.
[15] Morita RY. Bioavailability of energy and the starvation state. In: Starvation in bacteria. New York: Plenum Press; 1993. p. 1–24.
[16] Nystrom T. Oxidation of bacterial proteome in response to starvation. Methods Biochem Anal 2006;49:89–95.
[17] Zinser ER, Kolter R. Mutations enhancing amino acid catabolism confer a growth advantage in stationary phase. J Bacteriol 1999;181:5800–7.

[18] Matin A. The molecular basis of carbon-starvation-induced general resistance in Escherichia coli. Mol Microbiol 1991;5:3–10.
[19] Zhi-Wu W, Yong L, Jia-Qi Z, Yu L. The influence of short-term starvation on aerobic granules. Process Biochem 2006;41:2373–8.
[20] Khleifat KM. Biodegradation of phenol by *Ewingella americana*: effect of carbon starvation and some growth conditions. Process Biochem 2006;41:2010–6.
[21] Aakra A, Hesselsoe M, Bakken LR. Surface attachment of ammonia-oxidising bacteria in soil. Microb Ecol 2000;39:222–35.
[22] Lehman RM, Colwell FS, Bala GA. Attached and unattached microbial communities in a simulated basalt aquifer under fracture and porous-flow conditions. Appl Environ Microbiol 2001;67:2799–809.
[23] Ghiorse WC, Wilson JT. Microbial ecology of the terrestrial subsurface. J Adv Appl Microbiol 1988;33:107–72.
[24] Alvarez-Cohen L, McCarty PL. Effects of toxicity, aeration, and reductant supply on trichloroethylene transformation by a mixed methanotrophic culture. Appl Environ Microbiol 1991;57:228–35.
[25] Henry SM, Grbic-Galic D. Influence of endogenous and exogenous electron donors and trichloroethylene oxidation toxicity on trichloroethylene oxidation by methanotrophic cultures from a groundwater aquifer. Appl Environ Microbiol 1991;57:236–44.
[26] Jenkins RO, Heald SC. Stability of toluene oxidation by *Pseudomonas putida* under nutrient deprivation. Appl Microbiol Biotechnol 1996;46:388–92.
[27] Johnson DR, Park J, Kukor JJ, Abriola LM. Effect of carbon starvation on toluene degradation activity by toluene monooxygenase-expressing bacteria. Biodegradation 2006;17:437–45.
[28] Semprini L, McCarty PL. Comparison between model simulations and field results for in-situ biorestoration of chlorinated aliphatics: Part 2. Cometabolic transformations. Ground Water 1992;30:37–44.
[29] Park J, Chen YM, Kukor JJ, Abriola LM. Influence of substrate exposure history on biodegradation in a porous medium. J Contam Hydrol 2001;51: 233–56.
[30] Leahy JG, Olsen RH. Kinetics of toluene degradation by toluene-oxidizing bacteria as a function of oxygen concentration, and the effect of nitrate. FEMS Microbiol Ecol 1997;23:23–30.
[31] Olsen RH, Hansen J. Evolution and utility of a *Pseudomonas aeruginosa* drug resistance factor. J Bacteriol 1976;125:837–44.
[32] Weber Jr WJ, DiGiano FA. Process dynamics in environmental systems. New York: John Wiley and Sons; 1996. pp. 331–5.
[33] Byrne AM, Olsen RH. Cascade regulation of the toluene-3-monooxygenase operon (tbuA1UBVA2C) of *Burkholderia pickettii* PKO1: role of the rbuA1 promotor (PtbuA1) in the expression of its cognate activator, TbuT. J Bacteriol 1996;178:6327–37.
[34] Park J, Malinverni J, Adriaens P, Kukor JJ. Quantitative structure-activity relationship (QSAR) analysis of aromatic effector specificity in NtrC-like transcriptional activators from aromatic oxidizing bacteria. FEMS Microbiol Lett 2003;224:45–52.
[35] Link-field TG, Suflita JM, Tiedje JM. Characterization of the acclimation period before anaerobic dehalogenation of halobenzoates. Appl Environ Microbiol 1989;55:2773–8.
[36] de Smet MJ, Kingma J, Witholt B. The effect of toluene on the structure and permeability of the outer and cytoplasmic membranes of *Escherichia coli*. Biochim Biphys Acta 1978;506:64–80.
[37] Park J. Influence of substrate exposure history on biodegradation in porous media by *Ralstonia pickettii* PKO1. Ph.D. Dissertation. Ann Arbor: University of Michigan, 2002.